J. Fluid Mech. (1977), *vol.* 81, *part* 2, *pp.* 353–368
Printed in Great Britain

Steady flow in rapidly rotating variable-area rectangular ducts. Part 2. Small divergences

By A. CALDERON
Department of General Engineering, University of Puerto Rico, Mayaguez
AND J. S. WALKER
Department of Theoretical and Applied Mechanics, University of Illinois, Urbana

(Received 23 June 1976)

This paper treats the steady inertialess flow of an incompressible viscous fluid through an infinite rectangular duct rotating rapidly about an axis (the y axis) perpendicular to its centre-line (the x axis). The prototype considered has parallel sides at $z = \pm 1$ for all x, parallel top and bottom at $y = \pm a$ for $x < 0$ and straight diverging top and bottom at $y = \pm (a + bx)$ for $x > 0$. An earlier paper (Walker 1975) presented solutions for $b = O(1)$, for which the flow in the diverging part ($x > 0$) is carried by a thin, high-velocity sheet jet adjacent to the side at $z = 1$, the flow elsewhere in this part being essentially stagnant. The present paper considers the evolution of the flow as the divergence decreases from $O(1)$ to zero, the flow being fully developed for $b = 0$. This evolution involves four intermediate stages depending upon the relationship between b and E, the (small) Ekman number. In each successive stage, the flow-carrying side layer in the diverging part becomes thicker, until in the fourth stage, it spans the duct, so that none of the fluid is stagnant.

1. Introduction

The first part of this study (Walker 1975) treats the steady flow of an incompressible viscous fluid through a variable-area duct which has rectangular cross-sections and which is rotating rapidly about an axis perpendicular to its centre-line and parallel to one pair of its walls (the sides). The x axis coincides with the duct's centre-line and the y axis is parallel to the axis of rotation, so that $\boldsymbol{\omega} = \omega \hat{\mathbf{y}}$, where ω is the constant angular velocity and $\hat{\mathbf{y}}$ is a unit vector in the y direction. The flow is assumed to be inertialess, while the Ekman number $E = \nu/2\omega d^2$ is assumed to be small, so that viscous effects are confined to the boundary layers and free shear layers. Here ν is the fluid's kinematic viscosity, and d is half the distance between the sides, which are parallel for all ducts considered. Attention is focused on a prototype formed by joining a semi-infinite constant-area duct ($x < 0$) with walls at $y = \pm a$ and $z = \pm 1$ to a semi-infinite duct ($x > 0$) with parallel sides at $z = \pm 1$ and straight, symmetrically diverging top and bottom at $y = \pm (a + bx)$ (see figure 1). Far upstream ($x \to -\infty$), the flow is fully developed and the dimensionless axial velocity u is equal to one, except in the boundary layers. The fully developed flow is disturbed as it approaches the join. At the join, the flow enters a free shear layer of thickness $O(E^{\frac{1}{4}})$, which spans the duct at $x = 0$. Inside this layer, the entire flow turns towards the right-hand side (facing in the flow direction), so that the transverse velocity w must be large, $O(E^{-\frac{1}{4}})$, in order to carry the

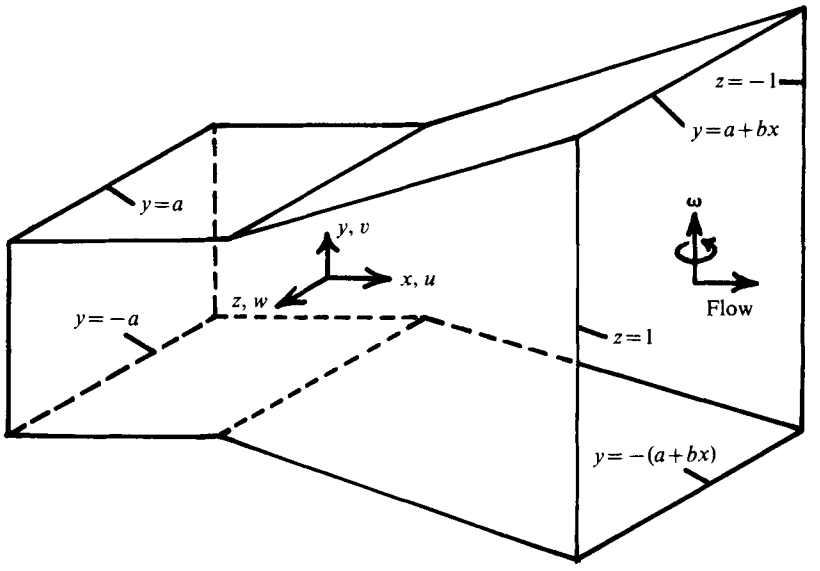

FIGURE 1. Duct.

$O(1)$ flow inside this thin layer. At $z = 1$, the flow turns back towards the $+x$ direction and enters a boundary layer of thickness $O(E^{\frac{1}{3}})$ adjacent to the right-hand side. In the diverging duct ($x > 0$), the entire flow is carried by a large, $O(E^{-\frac{1}{3}})$, axial velocity inside the boundary layer adjacent to the side $z = 1$, while the fluid elsewhere is essentially stagnant. For this solution, the inertialess approximation is valid if the Rossby number $Ro = U/2\omega d$ is much less than $E^{\frac{2}{3}}$, where U is the average velocity in the constant-area duct ($x < 0$).

The analysis presented in the previous part (Walker 1975) assumes implicitly that b, the slope of the top and bottom in the diverging duct ($x > 0$), is $O(1)$. However, if $b = 0$, the prototype is an infinite constant-area duct, and the flow is fully developed for all x. The object of the present analysis is to reconcile the radically different flows for $b = O(1)$ and $b = 0$ by considering the evolution of the flow as b decreases from $O(1)$ to 0. This evolution consists of four transitional stages:

$$(1)\, E^{\frac{1}{2}} \ll b \ll 1, \quad (2)\, b = O(E^{\frac{1}{2}}), \quad (3)\, E^{\frac{1}{2}} \ll b \ll E^{\frac{1}{2}}, \quad (4)\, b = O(E^{\frac{1}{2}}).$$

For the first three stages, the flow resembles that for $b = O(1)$. The disturbance to the fully developed flow in the constant-area duct ($x < 0$) is now $O(b)$ and is thus negligible. The flow enters the free shear layer of thickness $O(E^{\frac{1}{4}})$ at $x = 0$ and is again carried by an $O(E^{-\frac{1}{4}})$ transverse velocity inside this layer towards the right-hand side ($z = 1$). Here the flow turns and enters a boundary layer of thickness $O(\delta)$ adjacent to the side $z = 1$ in the diverging duct ($x > 0$), while the fluid outside this side layer in the diverging duct is still essentially stagnant. As b decreases, the side-layer thickness δ increases, and the order of magnitude of the large axial side-layer velocity, namely $O(\delta^{-1})$, decreases. Three different stages are required to cover this range of b because of changes in the relationship between the effects of the Coriolis force, viscosity and Ekman pumping. There are Ekman layers of thickness $O(E^{\frac{1}{2}})$ adjacent to the top and bottom

$$y = \pm(a + bx),$$

above and below the side layer. The variables in these Ekman layers match the side-layer variables as long as the normal components $(1+b^2)^{-\frac{1}{2}}(bu \mp v)$ of the side-layer velocity on the top and bottom $y = \pm(a+bx)$ equal the Ekman pumping, which is related to the normal component of the side-layer vorticity. For the first stage

$$E^{\frac{1}{2}} \ll \delta \ll E^{\frac{1}{4}},$$

and the Coriolis and viscous effects are comparable, while the Ekman pumping is negligible; for the second stage $\delta = O(E^{\frac{1}{4}})$, and all three effects are comparable; for the third stage $E^{\frac{1}{4}} \ll \delta \ll 1$, and the Coriolis force and the Ekman pumping are comparable, while the viscous effects in the side layer are negligible. For all three of these stages, the structure of the side layer is changing slowly in the x direction, so that $\partial/\partial x = O(b)$ in the diverging duct ($x > 0$).

As the slope approaches the fourth stage, $b = O(E^{\frac{1}{2}})$, the side-layer thickness δ becomes $O(1)$, so that the side layer is spreading across the entire duct and is evolving from a boundary layer into a core region. Alternatively, for $b \gg E^{\frac{1}{2}}$ the downstream core is a geostrophically blocked region, because the geostrophic surfaces $x =$ constant intersect the solid boundaries $z = \pm 1$, while for $b = O(E^{\frac{1}{2}})$ the downstream core is a geostrophically free region, because the top and bottom are very nearly parallel and there are no longer any geometrically defined geostrophic surfaces, so that the core can now carry the $O(1)$ flow. The structure of the free shear layer at $x = 0$ for $b \gg E^{\frac{1}{2}}$ is ultimately linked to the singular character of the solution in the intersections of the upstream and downstream Ekman layers at $x = 0$, $y = \pm a$. For $b = O(E^{\frac{1}{2}})$, these intersections no longer have singular solutions, and the free shear layer does not occur for this transitional stage.

In the fourth stage, the downstream core is divided into a near core for $0 \leqslant x < \infty$ in which $\partial/\partial x = O(1)$ and a far core for $0 < bx < \infty$ in which $\partial/\partial x = O(b)$. The far core represents the degenerate form of the right-hand side layer for $b \gg E^{\frac{1}{2}}$. While the flow in the far core is spread across the entire duct, the velocity profile in a horizontal plane is skewed towards the right-hand side as long as $b \neq 0$. The near core represents the degenerate form of the free shear layer at $z = 0$ for $b \gg E^{\frac{1}{2}}$. It accepts a uniform velocity profile at $x = 0$ and redistributes the flow towards the right-hand side in order to match the skewed far-core velocity profile as $x \to \infty$. As $b \to 0$ in the solution for the fourth stage, the dimensionless axial velocity in both the near and the far core approaches one, so that the flow becomes fully developed everywhere.

As b decreases through the four stages, the condition on the Rossby number under which the inertialess approximation is valid is relaxed, until in the fourth stage it becomes $Ro \ll 1$.

The flows treated here and in the first part of this study (Walker 1975) are closely related to the flows inside the impellers of centrifugal pumps and radial-flow hydraulic turbines, as well as to certain geophysical flows. In particular, since the β-effect on ocean currents is related to the effects of diverging walls and since the corresponding divergence would be relatively small, the present analysis may be of use in explaining certain oceanographic phenomena (Hseuh & Legeckis 1973).

2. General considerations

The flow considered here is incompressible, inertialess and steady relative to a Cartesian co-ordinate system which is rotating at a constant angular velocity $\boldsymbol{\omega} = \omega\hat{\mathbf{y}}$ relative to some inertial reference frame. The non-dimensional governing equations are

$$\nabla.\mathbf{v} = 0, \quad \hat{\mathbf{y}} \times \mathbf{v} = -\nabla\Phi + E\nabla^2\mathbf{v}, \tag{1a,b}$$

where $\mathbf{v}$ is the velocity, Φ is the reduced pressure, $\hat{\mathbf{y}}$ is a unit vector in the y direction and E is the Ekman number (Walker 1975). The flow is confined by a pair of semi-infinite rectangular ducts joined at $x = 0$ to give a prototype with sides at $z = \pm 1$ and with top and bottom at $y = \pm f(x)$, where

$$f = \begin{cases} a & \text{for} \quad x < 0, \\ a + bx & \text{for} \quad x > 0 \end{cases}$$

(see figure 1). The velocity $\mathbf{v}$ is normalized with respect to the average velocity in the constant-area duct ($x < 0$), so that the non-dimensional solution must satisfy the total-flow condition

$$\int_{-1}^{1} \int_{-f}^{f} u \, dy \, dz = 4a. \tag{2}$$

The boundary conditions are

$$\mathbf{v} = 0 \quad \text{at} \quad y = \pm f, \quad z = \pm 1, \tag{3a,b}$$

which, together with the governing equations (1), form a homogeneous problem whose solution is normalized by the condition (2).

If $E \ll 1$, the interior of the duct can be divided into an upstream core ($x < 0$), a downstream core ($x > 0$), a free shear layer of thickness $O(E^{\frac{1}{4}})$ which spans the duct at $x = 0$, boundary layers of various thicknesses adjacent to the sides $z = \pm 1$ and Ekman layers of thickness $O(E^{\frac{1}{2}})$ adjacent to the top and bottom $y = \pm f$. The well-known solutions for the Ekman layers satisfy the boundary conditions (3a) and match the variables in the adjacent core, free shear layer or side layer provided these variables satisfy the Ekman conditions at $y = \pm f$. For the present analysis, it turns out that $O(E^{\frac{1}{2}}b\nabla\mathbf{v})$ and $O(E^{\frac{1}{2}}\partial v/\partial y)$ terms are negligible, so that the Ekman conditions reduce to

$$f'u \mp v = (\tfrac{1}{2}E)^{\frac{1}{2}}(\partial u/\partial z - \partial w/\partial x) \quad \text{at} \quad y = \pm f, \tag{4}$$

where $f' = 0$ for $x < 0$ and $f' = b$ for $x > 0$ (Greenspan 1968, p. 92).

The present analysis treats the evolution of the flow from that treated in the first part of this study (Walker 1975), for which $b = O(1)$, to fully developed flow, for which $b = 0$. This evolution involves four transitional stages: (1) $1 \gg b \gg E^{\frac{1}{4}}$, (2) $b = O(E^{\frac{1}{4}})$, (3) $E^{\frac{1}{4}} \gg b \gg E^{\frac{1}{2}}$ and (4) $b = O(E^{\frac{1}{2}})$. The regions which carry the $O(1)$ flow, as well as sketches of the corresponding streamlines in the plane $y = 0$, are shown in figure 2 (a) for the first three stages and in figure 2 (b) for the fourth stage. For all four stages, the flow in the upstream core D is fully developed, so that

$$u = 1, \quad v = w = 0, \quad \Phi = z, \tag{5}$$

neglecting an $O(b)$ disturbance here (Calderon 1976). For the first three stages, the order of magnitude of the thickness δ of the downstream side layer A is (1) $(E/b)^{\frac{1}{2}}$, (2) $E^{\frac{1}{4}}$ and (3) $E^{\frac{1}{4}}/b$ respectively, while $\partial/\partial x = O(b)$ in this layer. For the fourth stage

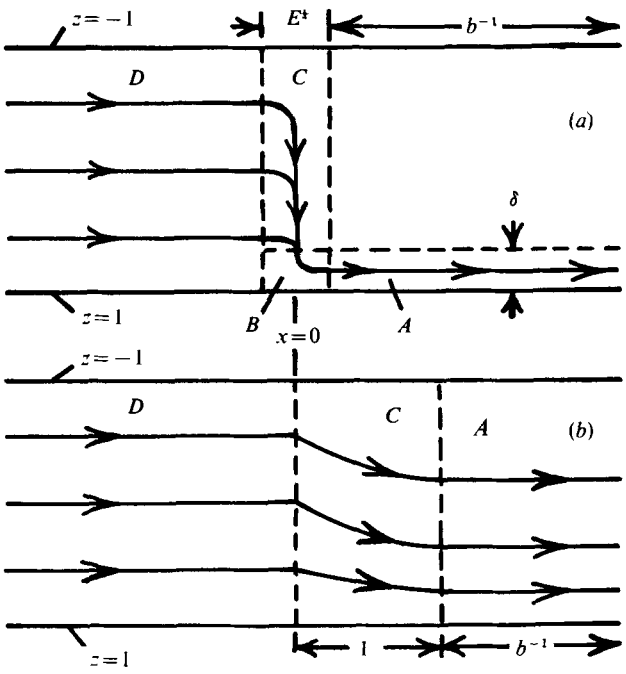

FIGURE 2. Horizontal sections at $y = 0$ showing the regions which carry the $O(1)$ flow and a sketch of the streamlines for (*a*) $1 \gg b \gg E^{\frac{1}{4}}$ (first three stages) and (*b*) $b = O(E^{\frac{1}{4}})$ (fourth stage).

$\partial/\partial x = O(1)$ in the near downstream core C and $\partial/\partial x = O(b)$ in the far downstream core A.

The objective here is an asymptotic solution for small b and E for four different relationships between b and E. In each flow-carrying region, the co-ordinates are stretched or compressed such that the gradient here is independent of E and b. The variables in this region are then written as asymptotic expansions in which the coefficients are functions of the possibly rescaled co-ordinates, but are independent of b and E. For the first and third stages b and E are independent small parameters, so that double asymptotic expansions are needed, e.g.

$$\begin{aligned} u = {} & \delta^{-1}u_{(0,0)} + u_{(1,0)} + \delta u_{(2,0)} + \dots \\ & + b\delta^{-1}u_{(0,1)} + bu_{(1,1)} + \dots \\ & + b^2\delta^{-1}u_{(0,2)} + \dots, \end{aligned}$$

while for the second and fourth stages there is only one independent small parameter, so that single expansions suffice, e.g.

$$u = E^{-\frac{1}{4}}u_{(0)} + u_{(1)} + E^{\frac{1}{4}}u_{(2)} + \dots .$$

Actually, perturbations with other powers of the small parameters enter these expansions through matching with adjacent regions, so that the expansions are not simple power series as shown above. However, whatever the irregular progression of the expansions, they can always be arranged into similar double expansions for stages 1 and 3 and single expansions for stages 2 and 4. The present analysis treats only the $O(1)$ flow and thus is concerned only with the leading terms in the asymptotic expan-

sions for each flow-carrying region. Henceforth $\mathbf{v}$ and Φ denote the leading terms in the expansions for these variables in one of the regions A, B and C.

Inertial effects are assumed to be negligible throughout, so that the inertial term $Ro(\mathbf{v}.\nabla)\mathbf{v}$ has been dropped from the Navier–Stokes equation to obtain (1*b*). Once the inertialess solution for a given stage has been found, the order of magnitude of the inertial term can be determined for the core, for each boundary layer and for the free shear layer at $x = 0$. Requiring that this term be much smaller than the terms in (1*b*) generates a condition on Ro for each subregion, and the most restrictive of these conditions for a given stage is the condition which must be satisfied for the entire flow to be inertialess. For $b = O(1)$, the most restrictive condition, $Ro \ll E^{\frac{2}{3}}$, follows from the high-velocity, downstream ($x > 0$) side layer at $z = 1$, in which the largest inertial forces occur. For small b, the governing condition always follows from the flow-carrying, downstream side layer (or core for the fourth stage). As the layer thickness increases and the layer velocity decreases with decreasing b, the inertialess condition is relaxed until, in the fourth stage, $Ro \ll 1$ is a sufficient condition. Such conditions could occur in centrifugal pumps or hydraulic turbines operating at design speed but with a very low flow rate. For a typical turbomachine operating under design conditions $E \ll 1$ but $Ro = O(1)$, so that the flow is not inertialess. For many geophysical flows both E and Ro are small, and many different relations between Ro and E occur in different physical situations.

Sections 2, 3, 4 and 5 present the solutions for stages 1, 2, 3 and 4 respectively. Many additional details, in particular the solutions for non-flow-carrying regions, are presented in Calderon's (1976) thesis.

3. First stage: $1 \gg b \gg E^{\frac{1}{4}}$

For small b, the solution presented in the first part of this study (Walker 1975) for the side layer of thickness $O(E^{\frac{1}{3}})$ at $z = 1$ in the diverging duct ($x > 0$) consists of a series of vanishing terms plus one term which dies out like $\exp[\frac{1}{2}(b/aE)^{\frac{1}{3}}(z-1)]$ far away from the side. This indicates that, as b decreases, the side-layer thickness δ increases and that, for $b \ll 1$, $\delta = O((E/b)^{\frac{1}{4}})$. That this is the correct expression for δ for the first stage is confirmed by the resulting solution. The lower limit on b for this stage follows from the Ekman condition (4). The right-hand side of this condition is negligible as long as $bu \gg E^{\frac{1}{2}}\delta^{-1}u = E^{\frac{1}{2}}b^{\frac{1}{2}}u$, or $b \gg E^{\frac{1}{4}}$.

With the change of co-ordinates $x = X/b$, $z = 1 + (E/b)^{\frac{1}{4}}\zeta$, equations (1) become

$$u = \partial\Phi/\partial\zeta, \quad v = y\partial^4\Phi/\partial\zeta^4 + F, \tag{6a, b}$$

$$w = \partial^3\Phi/\partial\zeta^3 - \partial\Phi/\partial X, \tag{6c}$$

where the orders of magnitude of u, v, w and Φ are δ^{-1}, $b\delta^{-1}$, b and 1 respectively, while Φ and F are integration functions of X and ζ only. The Ekman conditions (4) give $F = 0$ and

$$(a + X)\,\partial^4\Phi/\partial\zeta^4 + \partial\Phi/\partial\zeta = 0. \tag{7}$$

Consideration of (1) evaluated at the left-hand side wall $z = -1$, together with assumptions about the orders of magnitude of the variables and the derivatives in the neighbourhood of this side, indicates that the $O(1)$ term in Φ is constant along this side. The upstream core solution (5) indicates that $\Phi = -1$ along this side and throughout

the downstream core, since the fluid is essentially stagnant here. Therefore matching the downstream core gives the boundary condition

$$\Phi \to -1 \quad \text{as} \quad \zeta \to -\infty \tag{8}$$

on the $O(1)$ term in Φ in the downstream side layer A. There is a possibility of an inner side layer of thickness $O(E^{\frac{1}{3}})$ separating the outer side layer A from the side $z = 1$. Such a layer would have the same structure as a layer of thickness $O(E^{\frac{1}{3}})$ between the parallel top and bottom and therefore could not satisfy the condition (3*b*) and match non-zero values of either u or w in the outer side layer since these values would be independent of y (Howard 1969). Thus the solution of (7) must satisfy the boundary conditions

$$\partial\Phi/\partial\zeta = \partial^3\Phi/\partial\zeta^3 - \partial\Phi/\partial X = 0 \quad \text{at} \quad \zeta = 0. \tag{9a, b}$$

However, (6*b*), (7) and (9*a*) imply that $v = 0$ at $\zeta = 0$, so that the solution for the outer side layer A satisfies the boundary conditions (3*b*), and to first order no inner side layer is needed. The solution of (7) which satisfies the conditions (8) and (9) is

$$\Phi = A(a+X)^{-1}G - 1, \tag{10a}$$

where

$$G(X,\zeta) = \exp(Z)\,[\cos(c_1 Z) - \sin(c_1 Z)/c_1], \tag{10b}$$

$$Z = \zeta/2(a+X)^{\frac{1}{3}}, \quad c_1 = 3^{\frac{1}{2}}, \tag{10c, d}$$

A is an integration constant and the other variables are given by (6). Since the entire flow must be carried by this side layer, this solution must satisfy the condition (2), which gives $A = 2a$.

In this solution $\mathbf{v} = 0$ on the vertical surfaces $c_1 Z = -n\pi$, for $n = 0, 1, 2, \ldots$, and u is alternately positive and negative between these surfaces. Thus there are alternate layers of forward and backward flow with no $O(1)$ transfer of fluid between these layers. The boundary-layer thickness is growing like $(a+X)^{\frac{1}{3}}$, so that this layer spreads across the entire duct as $X \to \infty$. Indeed, as $X \to \infty$, the aspect ratio of the duct's cross-section approaches infinity, and the flow becomes Poiseuille flow between the sides. A separate analysis would be necessary in order to treat the development of the present side-layer solution into the solution for Poiseuille flow, and this analysis is not presented here. Consideration of the inertial perturbation of the present side-layer solution shows that the inertialess approximation is valid for this stage if $Ro \ll \delta^2 = (E/b)^{\frac{1}{3}}$ (Walker 1974).

The variables in the free shear layer C of thickness $O(E^{\frac{1}{4}})$ match the fully developed flow (5) upstream and the stagnant fluid downstream and deliver the entire flow to the intersection regon B. The slope b does not enter the governing equations, so that the solution here is given by a rescaling of similar solutions given by Howard (1969). The results are

$$u = \partial\Phi/\partial z, \quad v = -y\partial^4\Phi/\partial\xi^4, \quad w = -\partial\Phi/\partial\xi, \tag{11a, b, c}$$

$$\Phi = \begin{cases} \frac{1}{2}(1+z)\exp(-c_2\xi) - 1 & \text{for} \quad \xi > 0, \qquad (11d) \\ -\frac{1}{2}(1+z)\exp(c_2\xi) + z & \text{for} \quad \xi < 0, \qquad (11e) \end{cases}$$

where w is $O(E^{-\frac{1}{4}})$, while u, v and Φ are $O(1)$, and

$$\xi = E^{-\frac{1}{4}}x, \quad c_2 = 2^{-\frac{1}{4}}a^{-\frac{1}{4}}.$$

In this solution, v is discontinuous at $\xi = 0$, and there is an inner free shear layer of thickness $O(\mathrm{E}^{\frac{1}{3}})$ which separates the upstream ($\xi < 0$) and downstream ($\xi > 0$) halves

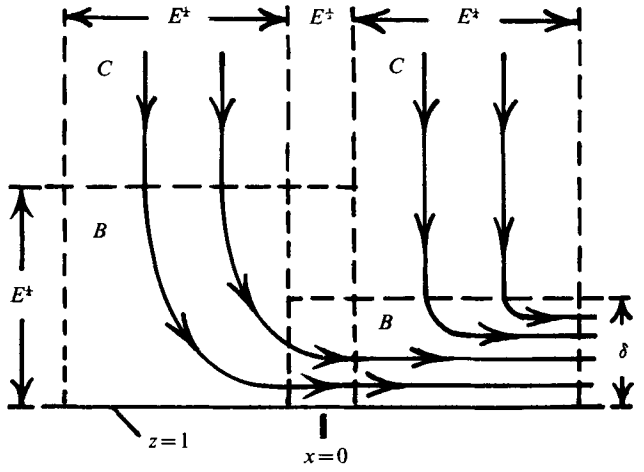

FIGURE 3. Intersection region B and streamlines in the plane $y = 0$ for the first stage, $1 \gg b \gg E^{\frac{1}{4}}$.

of the outer free shear layer C and which matches the two different values of v at $\xi = 0^{\pm}$. The solution for this inner layer is not presented here because this layer carries no $O(1)$ flow, but it is presented in Calderon's (1976) thesis.

Like the free shear layer C, the intersection region B is divided into an upstream half and a downstream half, separated by an inner region of thickness $O(E^{\frac{1}{4}})$ at $x = 0$. However, unlike the layer C, the two halves of region B have quite different structures arising from the difference in the Ekman conditions (4) with $f' = 0$ ($\xi < 0$) and with $f' = b$ ($\xi > 0$) (see figure 3). The transverse and axial dimensions of the downstream half are $O(\delta)$ and $O(E^{\frac{1}{4}})$ respectively, while the rescaled version of (1) gives

$$u = \partial\Phi/\partial\zeta, \quad v = -y\partial^4\Phi/\partial\zeta^4 + F, \quad w = -\partial\Phi/\partial\xi,$$

where the orders of magnitude of u, v, w and Φ are δ^{-1}, $b\delta^{-1}$, $E^{-\frac{1}{4}}$ and 1, respectively, while Φ and F are integration functions of ξ and ζ only. The Ekman conditions (4) give $F = 0$ and

$$a\partial^4\Phi/\partial\zeta^4 + \partial\Phi/\partial\zeta = 0,$$

which is the same as (7) with $X = 0$. As $\xi \to \infty$, the solution must match the downstream side-layer solution (10) evaluated at $X = 0$, while as $\zeta \to -\infty$, it must match the free-shear-layer solution (11) evaluated at $z = 1$. The boundary conditions (3b) become

$$\partial\Phi/\partial\zeta = \partial\Phi/\partial\xi = 0 \quad \text{at} \quad \zeta = 0,$$

which imply that v is zero here, as well as u and w. Therefore the solution is

$$\Phi = [\exp(-c_2\xi) - 1][1 - G(0,\zeta)] + G(0,\zeta).$$

For the upstream half of the intersection region B, the transverse and axial dimensions are both $O(E^{\frac{1}{4}})$, and (1) and the Ekman conditions (4) give

$$u = \partial\Phi/\partial\eta, \quad v = -c_2^2 y\nabla^2\Phi, \tag{12a, b}$$

$$w = -\partial\Phi/\partial\xi, \quad \nabla^4\Phi = c_2^2\nabla^2\Phi, \tag{12c, d}$$

where u and w are $O(E^{-\frac{1}{4}})$, while v and Φ are $O(1)$, Φ is an integration function of ξ and η only, so that ∇^2 is a two-dimensional Laplace operator, and

$$\eta = E^{-\frac{1}{4}}(z-1).$$

The boundary conditions are

$$\Phi \to 1-\exp(c_2\xi) \quad \text{as} \quad \eta \to -\infty, \tag{13a}$$

$$\Phi \to 1 \quad \text{as} \quad \xi \to -\infty, \tag{13b}$$

$$\Phi = 1, \quad \partial\Phi/\partial\eta = 0 \quad \text{at} \quad \eta = 0, \tag{13c, d}$$

$$\Phi = 0, \quad \partial\Phi/\partial\xi = -c_2 \quad \text{at} \quad \xi = 0. \tag{13e, f}$$

Here the condition (13a) arises from matching with the upstream half ($\xi < 0$) of the free-shear-layer solution (11); the condition (13b) arises from matching with the solution in the side layer of thickness $O(E^{\frac{1}{4}})$ at $z = 1$ in the constant-area duct ($x < 0$), in which the $O(1)$ term in Φ is unity since this layer carries no $O(1)$ flow; the conditions (13c, d) follow from the boundary conditions (3b) and the fact that the inner side layer of thickness $O(E^{\frac{1}{3}})$ here cannot accept a jump in u or w; the conditions (13e, f) follow from the continuity of u and w across the inner free shear layer of thickness $O(E^{\frac{1}{3}})$ at $x = 0$. On the other side of this inner free shear layer is the downstream half of the outer free shear layer C, evaluated at $z = 1$, rather than the other half of the intersection region B, since, relative to the upstream half of B, the downstream half has zero transverse dimension. Since the flow entering the upstream half of B must be passed on to the downstream half, it must all converge to the corner $\xi = \eta = 0$ in the upstream half. In fact, the jump in Φ from one at $\eta = 0$ for all ξ to zero at $\xi = 0$ for all η represents a line sink at the corner of the upstream half which absorbs half of the total flow through the duct. The boundary-value problem (12d) with (13) for the upstream half of the intersection region B is a well-posed, fourth-order, two-dimensional, elliptic problem on a quarter-plane. Solutions can be found using Fourier transform techniques, which lead to a singular integral equation, or by numerical techniques, such as a finite-difference relaxation scheme. Solutions are not presented here.

4. Second stage: $b = \alpha E^{\frac{1}{4}}$

As b for the first stage approaches $O(E^{\frac{1}{4}})$, the right-hand side of the Ekman conditions (4) for the downstream side layer A at $z = 1$ becomes comparable to the left-hand side, so that the effects of the Ekman pumping become comparable to those of the Coriolis force and viscosity, and the structure of this layer changes. For this stage, there is only one independent small parameter, taken to be $E^{\frac{1}{4}}$, while the other small parameter $b = \alpha E^{\frac{1}{4}}$, where α is a constant of proportionality which is independent of E. With the change of co-ordinates

$$x = E^{-\frac{1}{4}}X, \quad z = 1+E^{\frac{1}{4}}\zeta$$

for the side layer A, equations (1) again become equations (6), where now the orders of magnitude of u, v, w and Φ are $E^{-\frac{1}{4}}$, 1, $E^{\frac{1}{4}}$ and 1, respectively, while Φ and F are once again integration functions of X and ζ only. The Ekman conditions (4) now give $F = 0$ and

$$\partial^4\Phi/\partial\zeta^4 - 3p\partial^2\Phi/\partial\zeta^2 + 2q\partial\Phi/\partial\zeta = 0, \tag{14}$$

where

$$p(X) = 2^{-\frac{1}{2}}/3(a+\alpha X), \quad q(X) = \alpha/2(a+\alpha X).$$

The solution of (14) must satisfy the boundary conditions (8) and (9), since the downstream core is still essentially stagnant and the $O(1)$ term in Φ is -1 here, while the inner side layer of thickness $O(E^{\frac{1}{4}})$ at $z = 1$ cannot accommodate a jump in either u or w.

The characteristic polynomial for the differential equation (14) in ζ has four roots: one is zero, one is negative and two have positive real parts. The (real) negative root is excluded because the corresponding solution becomes unbounded as $\zeta \to -\infty$. For

$$X > X_0 = (2^{\frac{1}{2}}/27\alpha^2 - a)\,\alpha$$

the solution of (14) which satisfies the conditions (2), (8) and (9) is

$$\Phi = 2a(a+\alpha X)^{-1}\exp(r_1\zeta)\,[\cos(r_2\zeta) - r_1\sin(r_2\zeta)/r_2] - 1, \tag{15}$$

where $r_1 = s_+ + s_-, \quad r_2 = 3^{\frac{1}{2}}(s_- - s_+), \quad s_\pm = -\tfrac{1}{2}[-q \pm (q^2 - p^3)^{\frac{1}{2}}]^{\frac{1}{3}}.$

For $X < X_0$, the solution is

$$\Phi = 2a(a+\alpha X)^{-1}(r_+ - r_-)^{-1}[r_+\exp(r_-\zeta) - r_-\exp(r_+\zeta)]^{-1}, \tag{16}$$

where $r_\pm = 2p^{\frac{1}{2}}\cos[\tfrac{1}{3}(\theta \pm 2\pi)], \quad \theta = 2\pi + \arccos(-qp^{-\frac{3}{2}}).$

As $X \to X_0$, both of the solutions (15) and (16) become

$$\Phi = 18ra\alpha\exp(r\zeta)\,(1 - r\zeta) - 1,$$

where $r = r_+ = r_- = r_1 = 3\alpha/2^{\frac{1}{2}}, \quad r_2 = 0.$

As the slope parameter α decreases from large values, the characteristics of the solution for this stage evolve from those of the first-stage solution into those of the third-stage solution. For $\alpha > \alpha_0 = (2^{\frac{1}{2}}/27a)^{\frac{1}{2}}$, $X_0 < 0$, so that the solution (15) applies for all X. In the solution (15), $u = 0$ on the vertical surfaces $\zeta = -n\pi/r_2$ for $n = 0, 1, 2, \ldots$, and u is alternately positive and negative between these surfaces. Thus the side layer A involves alternate layers of forward and backward flow, just as it does for the first stage. For $\alpha < \alpha_0$, $X_0 > 0$, so that the solution (15) holds for $X > X_0$ and the solution (16) holds for $0 < X < X_0$. For $X > X_0$, there is still both forward and backward flow, but as $X \to X_0^+$, $r_2 \to 0$, and the position $\zeta = -\pi/r_2$ of the first surface where $u = 0$ tends to $-\infty$, so that $u > 0$ for all ζ at $X = X_0$.

In the solution (16) for $0 < X < X_0$, $u > 0$ for all ζ, so that there is no backflow here. As α decreases, X_0 increases, so that the length of the part of the side layer downstream of the join involving only forward flow increases. As $\alpha \to 0$, $X_0 \to \infty$, so that the side-layer flow is forward for all X and ζ.

In the solutions (15) and (16) for this stage, $v \neq 0$ at $\zeta = 0$, so that an inner side layer of thickness $O(E^{\frac{1}{4}})$ is needed to match this non-zero v and to satisfy the boundary conditions (3*b*). The solution in this inner layer is given by a local scaling of the solution for similar boundary layers between a parallel top and bottom (Howard 1969) and is not presented here. Consideration of the inertial perturbation shows that the inertialess assumption is valid for this stage if $Ro \ll \delta^2 = E^{\frac{1}{2}}$.

The structure of the free shear layer C at $x = 0$ is unchanged by the decrease in b to $O(E^{\frac{1}{4}})$, and the solution here is still given by (11). The axial and transverse dimensions of both the upstream ($\xi < 0$) and the downstream ($\xi > 0$) halves of the intersection region B are now $O(E^{\frac{1}{4}})$, i.e. $\delta = E^{\frac{1}{4}}$ in figure 3. In the upstream half, equations (12) and

boundary conditions (13*a–d*) still hold, with η now the same as ζ. In the downstream half, u and w, which are now $O(E^{-\frac{1}{4}})$, are given by (12*a*, *c*), while

$$v = -y\nabla^4\Phi,$$

$$\nabla^4\Phi - c_2^2\nabla^2\Phi + \alpha a^{-1}\partial\Phi/\partial\eta = 0, \tag{17}$$

where v and Φ are $O(1)$ and Φ is an integration function of ξ and η only. The solution of (17) must satisfy the boundary conditions

$$\Phi = 1, \quad \partial\Phi/\partial\eta = 0 \quad \text{at} \quad \eta = 0,$$

$$\Phi \to \exp(-c_2\xi) - 1 \quad \text{as} \quad \eta \to -\infty,$$

and as $\xi \to \infty$ it must match either (15) or (16) evaluated at $X = 0$, depending on whether $\alpha > \alpha_0$ or $\alpha < \alpha_0$, respectively. In addition, Φ and $\partial\Phi/\partial\xi$ evaluated at $\xi = 0^-$ in the upstream solution of (12*d*) must equal Φ and $\partial\Phi/\partial\xi$ evaluated at $\xi = 0^+$ in the downstream solution of (17), because of the continuity of u and w across the inner region which separates the two halves of the intersection region B. Two more conditions linking the solutions at $\xi = 0^{\pm}$ are needed in order for this pair of elliptic fourth-order equations with coupled boundary conditions to be a well-posed problem. Indeed, a detailed analysis of the inner region, whose axial and transverse dimensions are $O(E^{\frac{1}{2}})$ and $O(E^{\frac{1}{4}})$ respectively, yields two conditions relating the upstream and downstream values of $\partial^2\Phi/\partial\xi^2$ and $\partial^3\Phi/\partial\xi^3$ at $\xi = 0^{\pm}$ (Walker 1975). Solutions for the intersection region can be obtained by transform or numerical techniques, as before, but are not presented here.

5. Third stage: $E^{\frac{1}{4}} \gg b \gg E^{\frac{1}{2}}$

From (6*a*), and (16), the axial velocity in the downstream side layer A has the behaviour

$$u \to 2^{\frac{3}{4}}\alpha[\exp(2^{\frac{1}{4}}\alpha\zeta) - \exp(c_2\zeta)] \tag{18}$$

as $\alpha \to 0$. Since $$\alpha\zeta = (bE^{-\frac{1}{4}})E^{-\frac{1}{4}}(z-1) = bE^{-\frac{1}{4}}(z-1),$$

the first term in (18) indicates that the side-layer thickness for $b \ll E^{\frac{1}{4}}$ is given by $\delta = O(E^{\frac{1}{4}}/b)$, and this is confirmed by the resulting solution. The lower limit on b for this stage follows from setting $\delta = 1$, since then the assumption that this layer is a thin region no longer holds.

With the change of co-ordinates

$$x = X/b, \quad z = 1 + (E^{\frac{1}{4}}/b)\zeta,$$

equations (1) become $$u = \partial\Phi/\partial\zeta, \quad v = F, \quad w = -\partial\Phi/\partial X,$$

where the orders of magnitude of u, v, w and Φ are now δ^{-1}, $b\delta^{-1}$, b and 1, while Φ and F are integration functions of X and ζ only. Comparing these results with the results (6) for the first stage, the orders of magnitude are the same, although the definition of δ is different, while the viscous terms in (6*b*, *c*) are absent in the present expressions for v and w. The Ekman conditions (4) give $F = 0$ and

$$\partial^2\Phi/\partial\zeta^2 - 2^{\frac{1}{2}}\partial\Phi/\partial\zeta = 0. \tag{19}$$

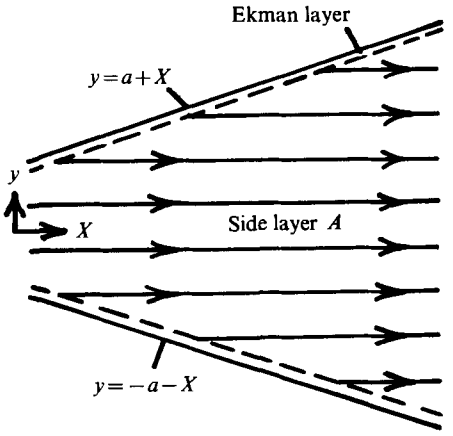

FIGURE 4. Streamlines in a vertical plane ζ = constant inside the downstream side layer A for the third stage, $E^{\frac{1}{4}} \gg b \gg E^{\frac{1}{3}}$.

The second term in (18) indicates that a side layer of thickness $O(E^{\frac{1}{4}})$ persists for $b \ll E^{\frac{1}{4}}$, but that the axial velocity here is $\delta^{-1} \ll E^{-\frac{1}{4}}$, so that this inner viscous layer carries no $O(1)$ flow. Thus the solution of (19) must satisfy the total-flow condition (2) and the condition (8), since the downstream core is still essentially stagnant. Thus the solution in the side layer A is

$$\Phi = 2a(a+X)^{-1}\exp(2^{\frac{1}{2}}\zeta) - 1. \tag{20}$$

Since $v = 0$, the streamlines in a plane ζ = constant must be horizontal, and since the top and bottom are diverging, all of the streamlines above $y = a$ and below $y = -a$ must originate from the Ekman layers at $y = \pm(a+X)$, as shown in figure 4. The flow entering the top and bottom of the side layer A from the adjacent Ekman layers in a section of length dX is $2a(a+X)^{-1}dX$. At $\zeta = 0$, $w = 2a(a+X)^{-2}$, so that the flow leaving the side layer and entering the inner side layer of thickness $O(E^{\frac{1}{4}})$ at $z = 1$ in the same section is also $2a(a+X)^{-1}dX$, and the total flow at each section of the side layer A is the same. Inside the inner side layer, the flow turns towards the top and bottom, where it enters the Ekman layers above and below the inner layer (see figure 5). Inside these Ekman layers, the flow turns away from the side $z = 1$ and enters the Ekman layers above and below the side layer A, where it turns once again towards the $+x$ direction and re-enters the side layer A. This transfer of flow is required in order to redistribute the side-layer flow as the top and bottom diverge in the absence of a vertical side-layer velocity. The inner side layer matches the non-zero values of u and w in the outer side layer A at $\zeta = 0$ and satisfies the boundary conditions $u = w = 0$ at $\eta = 0$, where, once again, $\eta = E^{-\frac{1}{4}}(z-1)$, but the solution for the inner side layer has a non-zero value of v at $\eta = 0$. An even thinner side layer with thickness $O(E^{\frac{1}{3}})$ matches this v and satisfies the boundary conditions (3b). The slope b does not enter the analysis of the inner side layers of thickness $O(E^{\frac{1}{4}})$ and $O(E^{\frac{1}{3}})$, and their structure is given by a local scaling of the structure of similar layers between a parallel top and bottom (Howard 1969). Consideration of the inertial perturbation to the solution for the side layer A for this stage indicates that the inertialess approximation holds as long as $Ro \ll \delta^2 = E/b^2$.

The structure of the free shear layer C at $x = 0$ remains unchanged by the decrease in

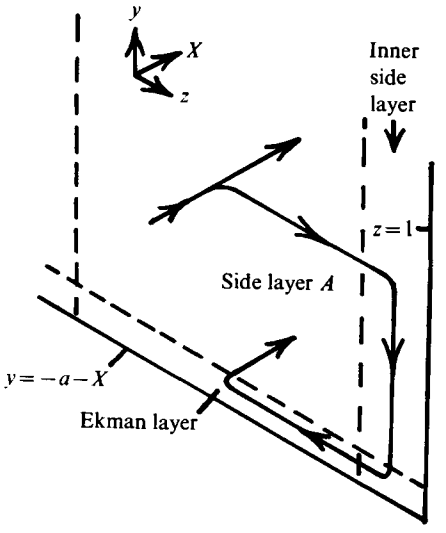

FIGURE 5. Isometric sketch showing transfer of flow from the central portion of side layer A through the inner side layer and Ekman layers to the bottom portion of side layer A for the third stage, $E^{\frac{1}{2}} \gg b \gg E^{\frac{1}{4}}$.

b to the range for this stage, and the solution here is still given by (11). The transverse and axial dimensions of the intersection region B are $O(\delta)$ and $O(E^{\frac{1}{2}})$ respectively. In this region, the $O(1)$ term in Φ is a function of ξ and ζ only, and the equation governing it, which is the same as the governing equation in the free shear layer C, involves only derivatives with respect to ξ. Therefore the solution can be found independently at each section ζ = constant. This solution is simply the local scaling of the solution (11) which gives $\Phi \to 1$ as $\xi \to -\infty$ and matches the solution in the side layer A evaluated at $X = 0$ as $\xi \to \infty$. The $O(E^{-\frac{1}{4}})$ term in w and the $O(1)$ term in v are still given by (11b, c) while the $O(\delta^{-1})$ term in u is given by $u = \partial\Phi/\partial\zeta$, and the solution for Φ is

$$\Phi = \begin{cases} 1 + H\exp(c_2\xi) & \text{for} \quad \xi < 0, \\ 1 + H[2 - \exp(-c_2\xi)] & \text{for} \quad \xi > 0, \end{cases}$$

where

$$H(\zeta) = \exp(2^{\frac{1}{2}}\zeta) - 1.$$

6. Fourth stage: $b = \mu E^{\frac{1}{2}}$

As b becomes $O(E^{\frac{1}{2}})$, δ for the third stage becomes $O(1)$, so that the side layer A evolves into a core region. For this stage, the downstream core is geostrophically free, so that the fluid here is no longer stagnant. Therefore there is no longer a need for a free shear layer C or an intersection region B to transfer the flow from the upstream core D to the downstream side layer A, and these regions do not occur in the first-order solution for this stage.

The downstream core ($x > 0$) is divided into a far core A, in which $\partial/\partial x = O(E^{\frac{1}{2}})$, and a near core C, in which $\partial/\partial x = O(1)$. With the change of co-ordinates $x = E^{-\frac{1}{2}}X$ for the far downstream core, (1) and the Ekman conditions (4) give

$$u = \partial\Phi/\partial z, \quad v = 0, \quad w = -\partial\Phi/\partial X, \tag{21a, b, c}$$

$$\partial^2\Phi/\partial z^2 - c_3\,\partial\Phi/\partial z = 0, \tag{21d}$$

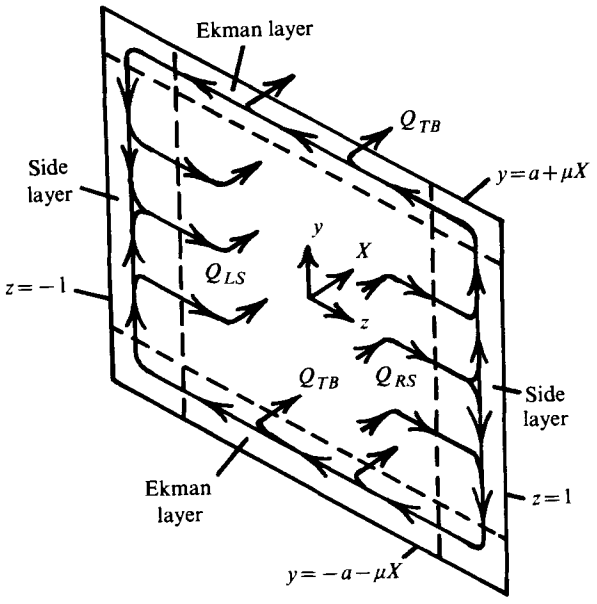

FIGURE 6. Isometric sketch showing circulation and redistribution of flow for the fourth stage, $B = O(E^{\frac{1}{4}})$.

where $c_3 = 2^{\frac{1}{2}}\mu$; u and Φ are $O(1)$; v and w are $O(E^{\frac{1}{2}})$; and Φ is a function of X and z only.

There are side layers of thickness $O(E^{\frac{1}{4}})$ which separate the downstream core from the sides at $z = \pm 1$. Since $u = O(1)$ in these layers, they make no contribution to the $O(1)$ flow, so that the solution of (21) must satisfy the total-flow condition (2). Therefore

$$\Phi = a(a+\mu X)^{-1}\,\mathrm{cosech}\,(c_3)\exp(c_3 z) + D,$$

where D is an integration function of X. The side layers of thickness $O(E^{\frac{1}{4}})$ match the non-zero core values of u and w at $z = \pm 1$ and satisfy the boundary conditions $u = w = 0$ at $\eta = 0$, where now $\eta = E^{-\frac{1}{4}}(z \mp 1)$ at $z = \pm 1$, as long as D is a constant. In the near-core solution, $\Phi = \pm 1$ at $z = \pm 1$ for all x, so that matching the near and far cores gives

$$D = -\coth c_3.$$

Like the solution for the downstream side layer A for the third stage, the present solution for the far downstream core A involves only horizontal streamlines, since $v = 0$, and yet the flow must be redistributed in the y direction as it progresses down the duct because of the divergence of the top and bottom. As in the third stage, this redistribution is accomplished through the transfer of flow from the core to the side layer of thickness $O(E^{\frac{1}{4}})$ at $z = 1$, then to the Ekman layers above and below this side layer, then to the Ekman layers above and below the core, and finally back into the core with a horizontal velocity at the top and bottom, thus maintaining a u which is independent of y. However, here we find an additional $O(E^{\frac{1}{4}})$ circulation of flow through the core, the side layers at $z = \pm 1$ and the Ekman layers at $y = \pm(a+\mu X)$. For a duct section of length dX, the total flow entering the right-hand side layer at $z = 1$ from the core is

$$Q_{RS} = 2\mu a(a+\mu X)^{-1}\,\mathrm{cosech}\,c_3 \exp c_3\, dX,$$

while the total flow entering the core from the Ekman layers at $y = \pm(a+\mu X)$ is

$$Q_{TB} = 4\mu a(a+\mu X)^{-1}dX.$$

The difference, namely

$$Q_{LS} = Q_{RS} - Q_{TB} = Q_{RS}\exp(2-c_3),$$

returns to the core from the left-hand side layer at $z = -1$, as shown in figure 6.

No change of co-ordinates is needed for the near core, and (1) and the Ekman conditions (4) give

$$u = \partial\Phi/\partial z, \quad v = 0, \quad w = -\partial\Phi/\partial x, \tag{22a, b, c}$$

$$\nabla^2\Phi - c_3\,\partial\Phi/\partial z = 0, \tag{22d}$$

where u, w and Φ are $O(1)$, v is $O(E^{\frac{1}{4}})$ and Φ is a function of x and z only, so that $\nabla^2 = \partial^2/\partial x^2 + \partial^2/\partial z^2$. The boundary conditions are

$$\Phi = z \quad \text{at} \quad x = 0, \quad \Phi = \pm 1 \quad \text{at} \quad z = \pm 1,$$

$$\Phi \to \operatorname{cosech} c_3 \exp(c_3 z) - \coth c_3 \quad \text{as} \quad x \to \infty,$$

which, together with (22*d*), represent a well-posed, two-dimensional, elliptic boundary-value problem. Analytic solutions can be found using separation of variables or Fourier transforms. Solutions are not presented here, but are presented in Calderon's (1976) thesis.

The solution for the fourth stage involves no free shear layers or large velocities in the side layers, and consideration of the inertial perturbation to this solution indicates that the inertialess approximation holds for the fourth stage as long as $Ro \ll 1$. As $\mu \to 0$, $\Phi \to z$, $u \to 1$ and $w \to 0$ in both the near and the far downstream core, so that the flow becomes fully developed for all x. This completes the transition from the flow treated in the first part of this study (Walker 1975), for which $b = O(1)$, to the fully developed flow for $b = 0$.

7. General duct geometries

The present analysis can be extended to more general duct geometries. If the top and bottom are at $y = \pm f(x)$, where $|f'| \ll 1$ for all x, while the sides remain parallel at $z = \pm 1$, then the duct can be subdivided axially into portions where

$$E^{\frac{1}{4}} \ll |f'| \ll 1, \quad |f'| = O(E^{\frac{1}{4}}), \quad E^{\frac{1}{4}} \ll |f'| \ll E^{\frac{1}{2}} \quad \text{or} \quad |f'| = O(E^{\frac{1}{2}}),$$

and the solution in each portion is given by a local scaling of the solution presented in §§ 2, 3, 4 or 5, respectively. This extension is considerably easier than the corresponding one for $|f'| = O(1)$, as discussed in the first part of this study (Walker 1975), because, to first order, the curvature of the top and bottom is negligible here. An exactly equivalent scaling is presented by Walker & Ludford (1972) for the analogous problem of an MHD flow in an insulated variable-area rectangular duct with a small divergence and with a strong transverse magnetic field. The extension to ducts with symmetrically diverging sides at $z = \pm g(x)$, with no restrictions on g, is discussed in the first part of this study (Walker 1975).

Hseuh & Legeckis (1973) present analytical and experimental results for a rapidly rotating rectangular duct with a straight converging bottom with an $O(E^{\frac{1}{4}})$ slope. Since

the present analysis neglects inertia, the solution in a converging duct can be obtained by simply changing the sign of the right-hand side of the total-flow condition (2). The solutions presented by Hseuh & Legeckis (1973) agree with solutions for the second stage, which are presented in §3, after the latter have been normalized to give flow in the $-x$ direction and the agreement between their analytical and experimental results tends to confirm the present analysis, as well as theirs. The results presented in §3 cover more possibilities for top and bottom slopes which are $O(E^{\frac{1}{4}})$ than those presented by Hseuh & Legeckis (1973), while the results presented in §§2, 4 and 5 provide the links between their results and the results for $b = O(1)$ and for $b = 0$.

This research was supported by the National Science Foundation under Grant ENG 74-23778.

REFERENCES

CALDERON, A. 1976 Steady flow in rapidly rotating rectangular ducts with small divergences. Ph.D. thesis, University of Illinois at Urbana-Champaign.

GREENSPAN, H. P. 1968 *The Theory of Rotating Fluids*. Cambridge University Press.

HOWARD, L. N. 1969 *Rotating Flow*. Lectures at the Royal Institute of Technology, Stockholm.

HSEUH, Y. & LEGECKIS, R. 1973 Western intensification in a rotating water tunnel. *Geophys. Fluid Dyn.* **5**, 333–358.

WALKER, J. S. 1974 Steady flow in rapidly rotating circular expansions. *J. Fluid Mech.* **66**, 657–671.

WALKER, J. S. 1975 Steady flow in rapidly rotating variable-area rectangular ducts. *J. Fluid Mech.* **69**, 209–227.

WALKER, J. S. & LUDFORD, G. S. S. 1972 Three-dimensional MHD duct flows with strong transverse magnetic fields. Part 4. Fully insulated, variable-area rectangular ducts with small divergences. *J. Fluid Mech.* **56**, 481–496.